Int J Cardiovasc Imaging (2013) 29:141–150
DOI 10.1007/s10554-012-0061-1

ORIGINAL PAPER

Reduced global longitudinal and radial strain with normal left ventricular ejection fraction late after effective repair of aortic coarctation: a CMR feature tracking study

Shelby Kutty · Sheela Rangamani · Jeeva Venkataraman · Ling Li · Andreas Schuster · Scott E. Fletcher · David A. Danford · Philipp Beerbaum

Received: 9 March 2012 / Accepted: 28 April 2012 / Published online: 12 May 2012

Abstract We sought to determine whether global and regional left ventricular (LV) strain parameters were altered in repaired coarctation of the aorta (COA) with normal LV ejection fraction (EF) when compared with healthy adult controls, and whether such alterations were related to LV hypertrophy (LVH). We identified 81 patients after COA repair (31 female, age 25 ± 8.5 years) with inclusion criteria at follow-up CMR of: age ≥13 years, time post-repair ≥10 years, no aortic valve disease, LV-EF >50 %). LV deformation indices derived using CMR-feature tracking and volumetric EF were compared between COA patients and normal controls (n = 20, 10 female, age 37 ± 7 years), and between COA with versus without LVH. In repaired COA versus controls, LV-EF (%) was 62 ± 7.2 versus 58 ± 3.0 ($p = 0.01$), and LV mass (g/m^2) 66 ± 16.8 versus 57.7 ± 6.0 ($p = 0.0001$). LV global longitudinal strain (GLS) was decreased to −17.0 ± 4.7 % in COA (−20 ± 5 % in controls, $p = 0.02$), and global radial strain (GRS) reduced to 40 ± 15 % (50 ± 12.4 % in controls, $p = 0.003$). The global circumferential strain (GCS) was preserved in COA at −23 ± 4.7 % (−24.6 ± 2.4 % in controls, $p = 0.14$). Regionally, LS decrease was marked in the basal segments (septal, p = 0.005, lateral, p = 0.013). In COA with LVH (n = 45, mass 76.3 ± 12.8 g/m^2) versus without LVH (n = 36, mass 52.2 ± 10 g/m^2), GLS was more markedly decreased (−15.7 ± 4.8 vs. −18.5 ± 4.2 %, $p = 0.016$, but GRS and GCS were similar ($p = 0.49$ and 0.27). In post-repair COA with normal LV-EF, GLS and GRS are reduced whilst GCS is preserved. GLS reduction is more pronounced in the presence of LVH. GLS may qualify as indicator of early LV dysfunction.

Keywords Adult congenital heart disease · Pediatric cardiology · Coarctation of the aorta · Cardiovascular magnetic resonance · Left ventricular mechanics · Feature tracking

Abbreviations

COA	Coarctation of the aorta
CHD	Congenital heart disease
CMR-FT	Cardiac magnetic resonance-feature tracking
LV	Left ventricle

Introduction

Coarctation of the aorta (COA) is a common lesion that accounts for 4–7 % of patients presenting with congenital heart disease (CHD) [1]. Patients born with COA typically receive surgical or transcatheter interventional therapy in infancy or childhood. Despite apparently successful relief of obstruction, late cardiovascular problems including systemic hypertension, left ventricular (LV) hypertrophy, heart

S. Kutty (✉) · S. Rangamani · J. Venkataraman · L. Li · S. E. Fletcher · D. A. Danford
Joint Division of Pediatric Cardiology, Children's Hospital and Medical Center, University of Nebraska College of Medicine/ Creighton University School of Medicine, 8200, Dodge Street, Omaha, NE 68114, USA
e-mail: skutty@unmc.edu

A. Schuster
Division of Imaging Sciences, King's College London British Heart Foundation Center of Excellence, National Institute of Health Research Biomedical Research Center at Guy's and St. Thomas' NHS Foundation Trust, The Rayne Institute, St. Thomas' Hospital, London, UK

P. Beerbaum
Department for Radiology and Pediatric Cardiology, Radboud University Nijmegen Medical Centre, Nijmegen, The Netherlands

failure, coronary heart disease, stroke and sudden cardiac death result in reduced life expectancy [2, 3].

There are relatively few data available regarding the effects of transcatheter and surgical treatments for COA on LV mechanics in the long term. Increased pump function [4, 5], as well as increased load-independent indexes of contractility [6, 7] have been reported after successful repair of COA in childhood. This would suggest alterations in ventricular performance long-term after successful repair, but the mechanisms responsible are incompletely understood. Conventional shortening and volumetric indices (e.g. ejection fraction, EF) quantify global pump function, but not the intrinsic myocardial contractile function [6].

Cardiovascular Magnetic Resonance (CMR) is increasingly used for non-invasive surveillance of adolescents and adults with repaired CHD because of its utility for evaluation of ventricular function and extracardiac thoracic vasculature. A CMR based feature-tracking (CMR-FT) method for quantitative assessment of cardiac mechanics has been recently introduced [8, 9]. This can be applied to standard vertical or horizontal long axis and mid ventricular short axis CMR images, allowing derivation of global and regional deformation using a semi-automatic myocardial tracking algorithm. CMR-FT is a relatively simple technique analogous to echocardiographic speckle tracking that does not require special image acquisition or complex post processing, and can be applied to previously acquired CMR images. Using CMR-FT, we have recently reported the feasibility of detecting quantitative changes in myocardial strain during dobutamine stress CMR [10]. The technique has been validated against harmonic phase myocardial tagging [8], and used to identify deformation abnormalities that correlated with myocardial scarring [11]. It has also shown promise in preliminary applications for CHD, including single ventricle [9] and repaired tetralogy of Fallot [12].

The aim of this study was to test the hypothesis that LV myocardial deformation indices measured by CMR-FT are altered in patients with repaired COA and normal LV EF, relative to healthy adult controls.

Methods

Patients

This was a single-center, retrospective observational study. Databases at the University of Nebraska Medical Center and Children's Hospital and Medical Center were reviewed to identify patients who had surgical or transcatheter treatment for COA and with the following inclusion criteria: (1) age $\geq$13 years, (2) CMR performed as part of clinical surveillance of repaired COA from 2006 to 2011, (3) EF on CMR >50 %, and (4) $\geq$10 years elapsed between treatment of COA and CMR evaluation. Studies in patients who had any cardiac lesion other than bicuspid aortic valve in association with COA (atrial septal defect, ventricular septal defect, subaortic stenosis, mitral valve disease at the time of COA repair or on follow up), or non-cardiac conditions (diaphragmatic hernia, chromosomal abnormalities including Turner's, DiGeorge, trisomies) were excluded. Patients with any grade of aortic stenosis and/or regurgitation were excluded based on most recent echocardiogram reports and aortic regurgitation fraction cutoff of 5 % on CMR phase contrast flow mapping. Patients who had evidence of recoarctation (defined as residual narrowing/diameter of descending aorta at the diaphragm $\leq$0.5) or aneurysm formation on CMR, and those who were on beta-blockers preceding the CMR were also excluded. Of 164 CMR studies performed for COA follow up, 94 met the inclusion criteria. Thirteen studies that did not have good quality images suitable for analysis were excluded yielding a study cohort of 81 patients. All selected studies had very good quality images suitable for analysis.

Demographic data of patients including age, gender, antihypertensive medication, aortic valve morphology (bicuspid vs. tricuspid), type of surgical (patch repair, subclavian flap arterioplasty, extended end-to-end repair, tube graft placement) or transcatheter (balloon angioplasty, stent angioplasty) interventions, and number of previous interventions were obtained. Twenty normal adult controls were recruited to derive normative CMR-FT data. The recruited controls were not currently active in competitive sports, had no history of cardiac or any other chronic illness, and were normotensive on the day of the study. The Institutional Review Board of the University of Nebraska Medical Center approved the study protocol and the normal controls recruited for the study signed informed consent.

Cardiac magnetic resonance imaging

CMR studies were performed on a 1.5 Tesla Philips Intera scanner (Philips Medical Systems, Best, The Netherlands). Ventricular dimensions and function were assessed with an electrocardiogram-gated steady state free-precession cine MR pulse sequence during brief periods of breath holding in the vertical long-axis (2-chamber), horizontal long-axis (4-chamber), and short-axis planes. The short axis plane was perpendicular to the ventricular long-axis based on the previous 4-chamber images, with 12–14 equidistant slices (slice thickness 6–8 mm; interslice space 0–2 mm) completely covering both ventricles. The CMR data was analyzed using commercially available computer workstation

(Extended MR work space version 2.6.3.2, Philips Medical Systems, Best, The Netherlands). The end-diastolic and end-systolic volumes, mass at end diastole, stroke volumes, and EF were measured for the LV using commercial software (View Forum, Philips Medical Systems). Ventricular end-diastolic volumes and mass were adjusted to body surface area using the Haycock formula. Each recruited control underwent quantitative CMR assessment from steady state free-precession cine images acquired at rest in the vertical long-axis, horizontal long-axis (4-chamber), and short-axis planes using the protocol as above.

CMR feature tracking

CMR cine images were analyzed offline by a single observer (JV) using 2D cardiac performance analysis-MR (2011 version, TomTec Imaging Systems, Unterschleissheim, Germany). Horizontal long axis and mid-ventricular short axis images were used for CMR-FT analysis. The horizontal long axis image was used to derive LV longitudinal strain and mid-ventricular short-axis slice containing both papillary muscles was used to obtain circumferential and radial strain. The software does allow analysis of each short axis image in a stack, however we chose to select the mid-ventricular slice to reduce potential tracking errors for the following reasons: (1) As radial strain measures wall thickening, the application of 2D tracking to measure radial strain is very sensitive to the chosen region of interest width, which can vary at the different slice levels; (2) the long axis (out-of-plane) motion of the heart, an issue that affects short axis tracking, is greater at the base than in the mid-ventricular level; and (3) consideration of the time required for analysis, and possible avoidance of redundant data. The right ventricular upper septal insertion point of the LV was manually detected to allow accurate segmentation in accordance with a standard model [13]. After placing points along the LV endocardium in a single frame, endocardial contours were manually drawn by one observer in all analyzed slices. This was followed by semi-automated feature tracking by the software. Multiple manual corrections were required in order to achieve good quality tracking. The software provided segmental and global values for velocity, displacement, and strain. Figure 1 shows a representative example of the tracking of LV in both views and the strain data obtained. Based on gender and body surface area specific nomograms published by Sarikouch et al. [14], the COA group was subdivided into those with normal indexed LV mass and increased indexed LV mass (defined as LV mass above the 97th percentile). A second observer (SK) repeated CMR-FT measurements in 15 randomly selected normal controls to assess interobserver variability.

Statistical analysis

All data are presented as means ± standard deviations or medians and ranges. Statistical comparisons were performed with a two-tailed unpaired Student's *t*-test. Strain data were compared between the COA group and normal controls, and between the COA subgroups with and without LV hypertrophy. Inter-observer variability was determined using Bland–Altman analysis to identify possible bias (mean divergence) and the limits of agreement (2 standard deviation of the divergence). A value of $p < 0.05$ was considered statistically significant. Statistical analysis was performed with the SPSS version 17.0.2 software package (SPSS Inc., Chicago, IL, USA) and MedCalc version 11.6.1 for Windows (MedCalc Inc., Mariakerke, Belgium).

Results

Demographic data and indices of global LV function in patients and normal controls are summarized in Table 1. Eighty-one patients were studied; the mean patient age was 24.9 ± 8.5 years. CMR examinations were performed at a mean of 16.5 ± 1.3 years after the first COA repair. Of the 81 patients, 52 had surgical repair of COA, 21 had balloon angioplasty, and information about previous intervention was unknown in 8. One patient had an additional surgical intervention after the primary surgical repair. Twenty-three patients had history of hypertension and 21 (26 %) of them were on antihypertensive medication (s) at the time of CMR examination. The antihypertensive regimen was at the discretion of the treating cardiologist and consisted of single or combination therapy with angiotensin converting enzyme inhibitor (enalapril, lisinopril, benazepril or fosinopril), angiotensin II receptor antagonist (losartan, valsartan), calcium channel blocker (amlodipine) or thiazide diuretic (hydrochlorothiazide). Two patients with mild hypertension were on no medications. Of 23 patients with history of hypertension, 19 had increased indexed LV mass on CMR. The LV EF and indexed LV mass were 61.8 ± 11.6 % and 65.7 ± 16.8 g/m^2 in the COA group. For the normal controls, LV EF was 57.5 ± 4.0 % and indexed mass 57.7 ± 6.0 g/m^2.

Global deformation indices

It was feasible to derive deformation indices for all subjects using CMR-FT. LV strain data from all patients with COA, the subgroups with normal (n = 36) and increased indexed LV mass (n = 45), and normal controls are summarized in Table 2. The LV global longitudinal (GLS), circumferential (GCS) and radial strains (GRS) in COA (%) were

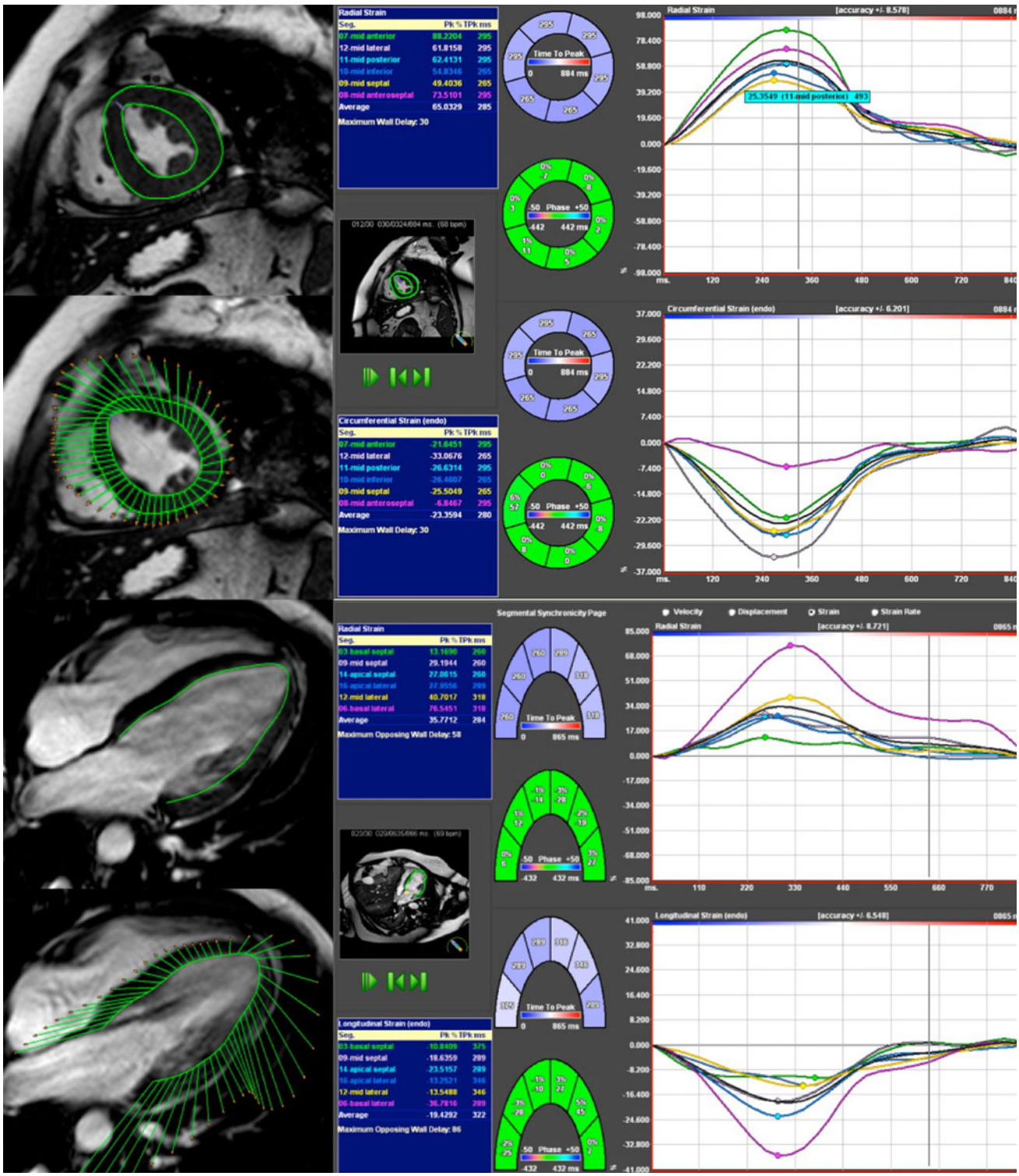

Fig. 1 Cardiac magnetic resonance feature tracking of the left ventricle in a patient with repaired coarctation of the aorta. *Top panels* show endocardial tracing and tracking in the short axis image with circumferential and radial strain curves (*right*) shown. *Bottom panels* show tracking from the four-chamber image to derive longitudinal strain

-17.0 ± 4.7, 23.0 ± 4.7 and 40.0 ± 15; the respective indices in controls (%) were -20 ± 5, -24.6 ± 2.4 and 50 ± 12.4. Compared to normal controls, the COA group showed decreased LV GLS ($p = 0.02$) and GRS, ($p = 0.003$). GCS strain tended to be lower in the COA group compared to controls, but this did not reach

Table 1 Demographics and global LV function in patients and controls

Variable	Normal adult controls (n = 20)		Repaired COA (n = 81)		COA with increased LV mass (n = 45)		COA with normal LV mass (n = 36)		COA with increased LV mass versus normal LV mass
	Mean ± SD	Range	Mean ± SD	Range	Mean ± SD	Range	Mean ± SD	Range	P value
Age at MRI (years)	37.1 ± 7.0	23.0–49.2	24.9 ± 8.2	13.4–50	17.8 ± 8.9	13.4–50	23.3 ± 7.1	14–43.4	0.265
Weight (kg)	72 ± 14.6	54.0–91.5	70.1 ± 18.1	30.4–118.0	66 ± 19.7	30.4–126.0	69.0 ± 16.1	46.0–108.8	0.463
Height (cm)	174.4 ± 7.0	154–189.0	171.0 ± 11.4	137.2–195.0	173.3 ± 11.7	137–193.0	168.0 ± 10.8	147.0–195.0	0.927
BSA (m^2)	1.85 ± 0.3	1.5–2.2	1.8 ± 0.3	1.2–2.4	1.8 ± 0.3	1.2–2.4	1.8 ± 0.2	1.4–2.3	0.336
COA repair (years)	NA	NA	6.0 ± 6.9	0.0–27.0	2.3 ± 7.9	0–27.0	4.1 ± 5.6	0–16.9	0.133
LV-EDVi (ml/m^2)	75.8 ± 12.7	58.5–102.0	81.1 ± 16.7	42.5–133.0	86.5 ± 16.7	40.5–133.0	71.8 ± 11.3	51.3–100.0	0.156
LV-mass (g/m^2)	57.7 ± 6.0	47.0–74.8	65.7 ± 16.8	43.0–113.0	76.3 ± 12.8	59.0–113	52.2 ± 10.	43.0–68.0	0.174
LV-EF (%)	57.5 ± 3.0	54.0–67.5	61.8 ± 7.2	50–89.0	63.4 ± 7.9	50.0–89.0	63.3 ± 6.5	52.0–77.0	0.694
LV-CI ($l/m/m^2$)	3.2 ± 0.6	2.9–3.8	3.4 ± 0.9	2.3–7.0	3.6 ± 1.1	2.3–7.0	3.2 ± 0.5	2.4–4.9	0.126

COA coarctation of the aorta, *LV* left ventricle, *BSA* body surface area, *EDVi* indexed end diastolic volume, *EF* ejection fraction, *CI* cardiac index, *NA* not applicable

statistical significance ($p = 0.14$). The LV GLS (%, mean ± standard deviation) was −15.7 ± 4.8 in the increased LV mass subgroup and −18.5 ± 4.2 in those with normal LV mass. Comparisons of strain between the subgroups with increased and normal LV mass showed decreased LV GLS ($p = 0.016$) in the former, whereas the differences in GCS and GRS did not reach statistical significance (Fig. 2). Compared to normal controls, the COA group with normal LV mass showed no significant difference in GLS ($p = 0.29$) and GCS ($p = 0.29$), but decreased GRS ($p = 0.04$). Representative examples of longitudinal strain curves in a normal adult control and in COA with and without LV hypertrophy are shown in Fig. 3.

Segmental deformation indices

Segmental indices of LV deformation derived from short axis and horizontal long axis steady state free precession cine are shown in Tables 3 and 4. The decrease in longitudinal strain was marked in the basal segments of the LV; mean basal septal and basal lateral segmental strains in COA (%) were −14.3 and −19.5, while corresponding segmental strains in normal controls (%) were −22.6 and −27.0. Radial strain displayed significant regional heterogeneity in COA, with higher values in the septal and anteroseptal segments and lower values in the remaining segments, as compared to controls.

Bland–Altman analysis showed good agreement between observers for GLS and GCS, and higher variability for GRS (Fig. 4). The reproducibilities for GLS, GCS, and GRS measurements were 97.8, 97.5 and 95.6 % respectively. The respective degrees of bias for GLS, GCS and GRS were −1.57, −0.01 and −0.32 and the limits of agreement were −0.32 ± 2.14, −0.01 ± 3.41 and −1.57 ± 10.8. A sub-analysis was performed to explore the relation between (a) the age at COA treatment and (b) the type of treatment with the presence of LV hypertrophy. No statistically significant associations were found; the respective p values were 0.184 (the type of repair vs. LV mass) and 0.300 (LV mass in patients treated <1 year vs. >1 year of age).

Discussion

Patients after COA repair are prone to significant late cardiovascular abnormalities that may cause important morbidity and mortality. Systemic hypertension is common and can lead to ventricular hypertrophy, premature atherosclerosis and coronary heart disease [15]. In this context, CMR is a well-established and cost-effective modality to follow up COA repair [16, 17] and considered the

Table 2 Global LV strains in patients and controls

	COA	Normal Controls	COA with increased LV mass	COA with normal LV mass
Radial strain (%)	40.0 ± 15.2	50 ± 12.4	38.8 ± 12.9	41.2 ± 17.8
Circumferential strain (%)	−23.0 ± 4.7	−24.6 ± 2.4	−22.5 ± 5.0	−23.7 ± 4.2
Longitudinal strain (%)	−17.0 ± 4.7	−20.0 ± 5.1	−15.7 ± 4.8	−18.5 ± 4.2

COA coarctation of aorta, *LV* left ventricle

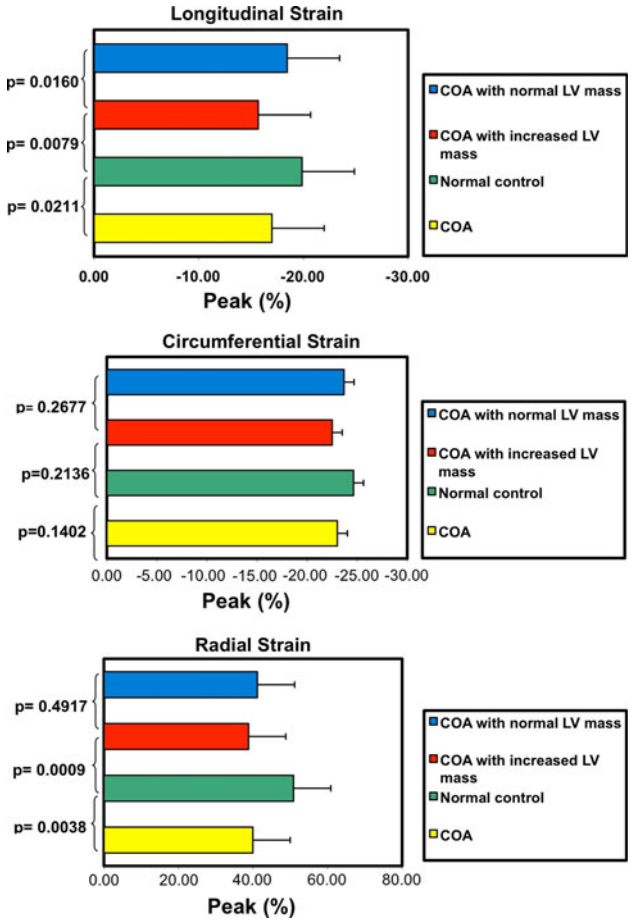

Fig. 2 Comparisons of global longitudinal (*top panel*), circumferential (*middle panel*) and radial (*lower panel*) strains between patients with coarctation and normal controls, and between the subgroups of coarctation with and without left ventricular hypertrophy

present day reference standard for assessment of ventricular function [16].

Study findings

This is the first report of quantifying LV myocardial deformation in COA from standard CMR images routinely performed to assess LV function. All three principal patterns of LV deformation: longitudinal, circumferential and radial were studied. Importantly, we found evidence that even in the presence of a normal LV systolic function; the GLS and GRS were significantly reduced when compared with healthy controls. Although this observation was made for the whole population of patient post COA repair, the reduction of GLS was even more obvious in those patients with LV hypertrophy. Despite reduction in LV GLS and GRS, GCS in COA remained reasonably well preserved.

Altered LV mechanics after COA repair

Altered LV function has been observed in children years after COA repair by 2-dimensional echocardiography [4]. Greater fractional shortening, peak shortening velocity, and increased LV mass are reported after COA repair relative to healthy controls [4]. Diastolic filling abnormalities occur in association with increased systolic blood pressure and LV mass index [4]. Increased LV contractility manifested as increased wall stress to rate-corrected velocity of shortening has also been identified in a significant number of patients after COA repair [7].

Standard volumetric indices such as LV EF provide a global assessment of LV function, but do not indicate intrinsic contractile function. On the other hand, indices of myocardial deformation (strain and strain rate) have been shown to detect early myocardial abnormalities and contractile dysfunction [18, 19]. In an echocardiographic study of patients with impaired LV systolic function, Stanton et al. have identified GLS as a superior predictor of outcome to either EF or wall motion score index and suggested that GLS may become the optimal method for assessment of global LV systolic function [20]. Moreover, late after repair in tetralogy of Fallot with normal LV EF, Kempny et al. have observed that two dimensional echocardiography derived GLS is significantly reduced, suggesting subclinical LV myocardial dysfunction [21]. The value of strain imaging has also been suggested in COA and in aortic stenosis, both conditions with increased LV afterload [19, 22]. Impaired longitudinal deformation was shown after COA repair that correlated with the age at repair and systolic blood pressure, and this matches our observations [22, 23]. Others have noted decreased segmental and GLS in both children and adults with aortic stenosis [18, 19, 24]. Another index of deformation, LV torsion, is increased as compensatory adaptation to increased pressure load [24].

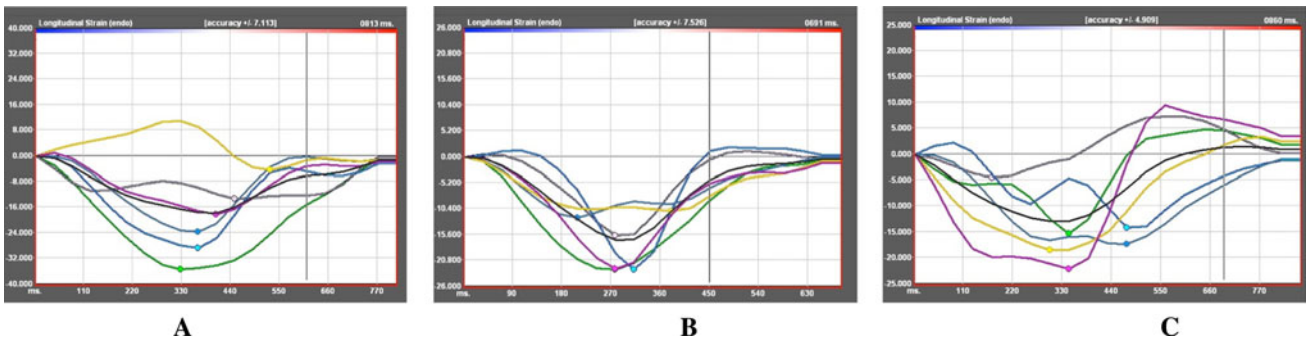

Fig. 3 Representative examples of segmental and global longitudinal strain curves in a normal adult control (**a**), coarctation with normal LV mass (**b**) and coarctation with LV hypertrophy (**c**) are shown. The respective values (%) for global longitudinal strain in **a**, **b** and **c** were −19.7, −16.4 and −12.8

Changes in deformation with ventricular hypertrophy

It is noteworthy that in our COA population GLS was significantly more reduced in the presence of LVH (compared to normal LV mass), whereas GCS and GRS were similar. Hence it could be speculated that deformation in the LV subendocardial longitudinal fibers may be more affected, relative to subepicardial and circumferential midwall fibers. Alterations in LV GLS with preservation of radial and circumferential deformation like those reported here, have been described in systemic hypertension, suggesting that this abnormal pattern of LV deformation results from afterload induced myocardial hypertrophy. In contrast, others have found a compensatory increase in radial function in patients with LV hypertrophy [25], perhaps responsible for their hyperdynamic EF measurements.

LV hypertrophy allows preserved EF and normal fiber shortening at the endocardium despite decreased longitudinal fiber shortening [26], but hypertrophy is also associated with decreased capillary density [27]. Hypertrophy associated altered coronary flow reserve [28, 29] may contribute to LV dysfunction in the long term. However, in the setting of repaired COA, additional factors likely contribute to myocardial structural changes, and require further investigation. For example, changes in central aortic and conduit vessel compliance and abnormal ventriculoarterial coupling are known to alter LV load [30]. Reduced proximal aortic strain and increased stiffness are seen after COA repair, which may also contribute to hypertension and increased LV burden [31].

Late hypertension is common despite successful repair of COA, and its reported prevalence varies depending on the diagnostic criteria used. Importantly, hypertension often recurs during long-term follow up. Though the prevalence of late hypertension is likely related to the age at COA repair and to the duration of follow-up as has been previously shown, the exact etiology is unknown. Several theories have been proposed, including abnormal aortic compliance, neuroendocrine activation, and abnormal baroreceptor function. In some patients, despite normal resting values, blood pressure abnormalities such as elevated values on ambulatory monitoring, decreased diurnal variation, and abnormal response to exercise have been demonstrated. Undoubtedly, a combination of factors is likely responsible, and our data is inadequate to draw definitive conclusions.

CMR-FT in comparison with other modes of deformation imaging

Two-dimensional echocardiography derived LV GLS has been shown to have superior incremental prognostic value over conventional measures of LV systolic function [20]. Most studies on deformation assessment have utilized echocardiography, the accuracy of which is dependent on two-dimensional image quality. Higher temporal resolution of two-dimensional echocardiography is an advantage over CMR, however greater signal to noise ratio makes CMR-FT potentially superior to echocardiography in image quality and border tracking. CMR-FT enables derivation of global and segmental myocardial deformation from standard cine CMR. Therefore, as in our study, a comprehensive analysis of myocardial function and mass can be combined into a single modality. LV GLS had the best interobserver agreement, followed by GCS, while GRS showed wider degrees of divergence between observers. This pattern is very similar to reports of interobserver agreement in the echocardiography literature. Myocardial tagging is an alternative CMR tool for deformation assessment that has been shown to be feasible in adults with aortic stenosis [23, 32], but involves special image acquisition (with inherent dependency on the contrast between the tag lines and the myocardium), and more demanding post-processing not associated with CMR-FT.

Table 3 LV segmental deformation in coarctation versus normal controls: (short axis)

	Mid anterior		Mid lateral		Mid posterior		Mid inferior		Mid septal		Mid anteroseptal	
	COA[b]	Normal control	COA	Normal control	COA	Normal control	COA	Normal control	COA	Normal control	COA	Normal control
Radial velocity (cm/s)	3.4 ± 0.8	3.6 ± 0.7	3.2 ± 0.9	3.5 ± 0.6	3.2 ± 0.9	3.8 ± 0.9	3.2 ± 0.9	3.8 ± 0.9	3.2 ± 0.9	3.3 ± 0.7	3.3 ± 0.9	3.3 ± 0.7
Radial displacement (mm)	6.8 ± 1.6	7.2 ± 1.0	6.2 ± 1.6	6.8 ± 0.9	6.4 ± 1.6	7.2 ± 1.2	6.7 ± 1.5	7.5 ± 1.4	6.2 ± 1.5	6.5 ± 1.5	6.3 ± 1.6	6.3 ± 1.6
Radial strain (%)	42.6 ± 19.6	63.7 ± 22.0	50.7 ± 24.4	59.4 ± 16.1	49.4 ± 22.9	50.7 ± 19.4	40.8 ± 19.2	49.5 ± 18.4	28.6 ± 15.1	21.6 ± 12.9	29.1 ± 16.2	24.4 ± 10.7
Circumferential strain (%)	−23.3 ± 8.6	−20.7 ± 5.1	−23.6 ± 9.0	−26.1 ± 6.9	−22.3 ± 7.4	−29.2 ± 5.2	−22.8 ± 7.5	−24.1 ± 8.5	−23.0 ± 7.3	−24.1 ± 6.2	−22.8 ± 7.7	−23.7 ± 5.4

LV left ventricle, *COA* coarctation of aorta

Table 4 LV segmental deformation in coarctation versus normal controls (horizontal long axis)

	Basal septal		Mid septal		Apical septal		Apical		Mid		Basal lateral	
	COA	Normal control	COA	Normal control	COA	Normal control	COA	Normal control	COA	Normal control	COA	Normal control
Longitudinal velocity(cm/s)	3.8 ± 2.0	4.8 ± 1.8	3.3 ± 1.7	3.7 ± 1.3	1.8 ± 0.8	2.1 ± 1.3	2.5 ± 1.4	2.9 ± 1.6	3.9 ± 1.9	3.9 ± 1.7	4.1 ± 1.8	4.3 ± 1.6
Longitudinal displacement (mm)	6.0 ± 3.0	8.3 ± 3.6	4.6 ± 2.5	4.7 ± 2.4	2.0 ± 1.3	2.3 ± 1.2	3.5 ± 2.0	2.6 ± 1.6	5.8 ± 3.1	3.8 ± 2.5	6.5 ± 3.4	6.4 ± 3.4
Longitudinal strain (%)	−14.3 ± 8.0	−22.6 ± 9.0	−12.4 ± 7.3	−14.5 ± 8.0	−22.0 ± 8	−19.6 ± 7.3	−20.1 ± 9.1	−18.5 ± 8.5	−13.9 ± 7.4	−18.0 ± 9.0	−19.5 ± 9.0	−27.0 ± 12.8

LV left ventricle, *COA* coarctation of aorta

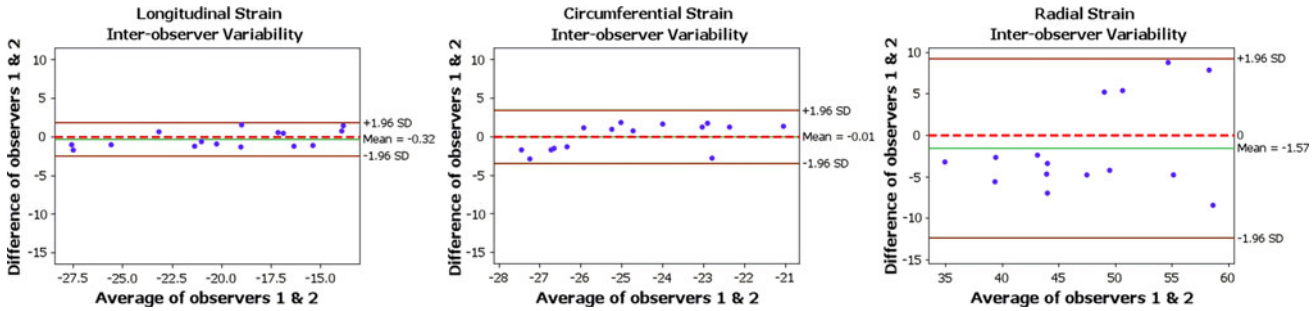

Fig. 4 Bland–Altman plots for inter-observer agreement of global longitudinal, circumferential and radial strains with differences plotted against mean values for each measurement

Study limitations

This study has several limitations. Though non-invasive blood pressure gradients were obtained during yearly clinic visits in our study cohort, simultaneous blood pressure data were not available with CMR. Thus, the available data does not allow us to sort out the importance of this confounding variable on the altered LV mechanics. It is possible that all the changes in strain uncovered in this work may be primarily related to the presence of systemic hypertension rather than the late effects of COA repair. Athletes were excluded from the control group, and the controls were not age and gender matched. This yielded a somewhat older control group, which did not include a potentially useful subgroup of patients with physiologic hypertrophy (competitive athletes). The relatively small numbers of patients with LV hypertrophy precluded meaningful exploration for correlations of decreased strain with myocardial late enhancement, a well-studied CMR marker for myocardial fibrosis. Prior to routine application of CMR-FT in children with COA, derivation of normal ranges for deformation indices in the pediatric age group is necessary considering age, gender and allometry. Finally, the study design did not permit correlation of measurements of deformation with clinical outcomes.

Conclusions

CMR-FT allowed quantification of global and segmental LV mechanics and changes with LV hypertrophy in young adults long-term after aortic COA repair. Reduced global longitudinal and radial strains were found with normal LV EF late after effective repair. LV deformation indices are potentially useful in the clinical follow up of COA, with LV global longitudinal strain showing promise as a robust index. Further studies are necessary to evaluate the relationship between LV deformation indices and clinical outcomes in patients after COA treatment.

Acknowledgments The authors appreciate the assistance of the Magnetic Resonance Imaging laboratory staff at the Children's Hospital and Medical Center. We also thank Berthold Klas, BS, TomTec Imaging Systems, TomTec Corporation USA for technical assistance. SK receives support from the American College of Cardiology Foundation and the American Heart Association.

Conflict of interest None.

References

1. Fixler DE, Pastor P, Chamberlin M, Sigman E, Eifler CW (1990) Trends in congenital heart disease in Dallas County births 1971–1984. Circulation 81:137–142
2. Cohen M, Fuster V, Steele PM, Driscoll D, McGoon DC (1989) Coarctation of the aorta. Long-term follow-up and prediction of outcome after surgical correction. Circulation 80(4):840–845
3. Toro-Salazar OH, Steinberger J, Thomas W, Rocchini AP, Carpenter B, Moller JH (2002) Long-term follow-up of patients after coarctation of the aorta repair. Am J Cardiol 89:541–547
4. Moskowitz WB, Schieken RM, Mosteller M, Bossano R (1990) Altered systolic and diastolic function in children after "successful" repair of coarctation of the aorta. Am Heart J 120: 103–109
5. Kimball T, Reynolds J, Mays W, Khoury P, Claytor R, Daniels SR (1994) Persistent hyperdynamic cardiovascular state at rest and during exercise in children after successful repair of coarctation of the aorta. J Am Coll Cardiol 24:194–200
6. Gentles TL, Sanders SP, Colan SD (2000) Misrepresentation of left ventricular contractile function by endocardial indexes: clinical implications after coarctation repair. Am Heart J 140: 585–595. doi:10.1067/mhj.2000.109642
7. Leandro J, Smallhorn JF, Benson L, Musewe N, Balfe JW, Dyck JD, West L, Freedom R (1992) Ambulatory blood pressure monitoring and left ventricular mass and function after successful surgical repair of coarctation of the aorta. J Am Coll Cardiol 20:197–204
8. Hor KN, Gottliebson WM, Carson C, Wash E, Cnota J, Fleck R, Wansapura J, Klimeczek P, Al-Khalidi HR, Chung ES, Benson DW, Mazur W (2010) Comparison of magnetic resonance feature tracking for strain calculation with harmonic phase imaging analysis. JACC Cardiovasc Imaging 3:144–151. doi:10.1016/j.jcmg.2009.11.006
9. Truong UT, Li X, Broberg CS, Houle H, Schaal M, Ashraf M, Kilner P, Sheehan FH, Sable CA, Ge S, Sahn DJ (2010) Significance of mechanical alterations in single ventricle patients on

twisting and circumferential strain as determined by analysis of strain from gradient cine magnetic resonance imaging sequences. Am J Cardiol 105:1465–1469. doi:10.1016/j.amjcard.2009.12.074
10. Schuster A, Kutty S, Padiyath A, Parish V, Gribben P, Danford DA, Makowski MR, Bigalke B, Beerbaum P, Nagel E (2011) Cardiac magnetic resonance myocardial feature tracking detects quantitative wall motion during dobutamine stress. J Cardiovasc Magn Reson 13:58
11. Schuster A, Paul M, Bettencourt N, Morton G, Chiribiri A, Ishida M et al (2011) Cardiovascular magnetic resonance myocardial feature tracking for quantitative viability assessment in ischemic cardiomyopathy. Int J Cardiol
12. Ortega M, Triedman JK, Geva T, Harrild DM (2011) Relation of left ventricular dyssynchrony measured by cardiac magnetic resonance tissue tracking in repaired tetralogy of fallot to ventricular tachycardia and death. Am J Cardiol 107:1535–1540. doi:10.1016/j.amjcard.2011.01.032
13. Cerqueira MD, Weissman NJ, Dilsizian V, Jacobs AK, Kaul S, Laskey WK, Pennell DJ, Rumberger JA, Ryan T, Verani MS (2002) Standardized myocardial segmentation and nomenclature for tomographic imaging of the heart: a statement for healthcare professionals from the Cardiac Imaging Committee of the Council on Clinical Cardiology of the American Heart Association. Circulation 105:539–542
14. Sarikouch S, Peters B, Gutberlet M, Leismann B, Kelter-Kloepping A, Koerperich H, Kuehne T, Beerbaum P (2010) Sex-specific pediatric percentiles for ventricular size and mass as reference values for cardiac MRI: assessment by steady-state free-precession and phase-contrast MRI flow. Circ Cardiovasc Imaging 3:65–76. doi:10.1161/circimaging.109.859074
15. de Divitiis M, Rubba P, Calabro R (2005) Arterial hypertension and cardiovascular prognosis after successful repair of aortic coarctation: a clinical model for the study of vascular function. Nutr Metab Cardiovasc Dis 15:382–394
16. Kilner PJ, Geva T, Kaemmerer H, Trindade PT, Schwitter J, Webb GD (2010) Recommendations for cardiovascular magnetic resonance in adults with congenital heart disease from the respective working groups of the European Society of Cardiology. Eur Heart J 31:794–805
17. Therrien J, Thorne SA, Wright A, Kilner PJ, Somerville J (2000) Repaired coarctation: a "cost-effective" approach to identify complications in adults. J Am Coll Cardiol 35:997–1002
18. Iwahashi N, Nakatani S, Kanzaki H, Hasegawa T, Abe H, Kitakaze M (2006) Acute improvement in myocardial function assessed by myocardial strain and strain rate after aortic valve replacement for aortic stenosis. J Am Soc Echocardiogr 19:1238–1244. doi:10.1016/j.echo.2006.04.041
19. Poulsen SH, Sogaard P, Nielsen-Kudsk JE, Egeblad H (2007) Recovery of left ventricular systolic longitudinal strain after valve replacement in aortic stenosis and relation to natriuretic peptides. J Am Soc Echocardiogr 20:877–884. doi:10.1016/j.echo.2006.11.020
20. Stanton T, Leano R, Marwick TH (2009) Prediction of all-cause mortality from global longitudinal speckle strain: comparison with ejection fraction and wall motion scoring. Circ Cardiovasc Imaging 2:356–364. doi:10.1161/CIRCIMAGING.109.862334
21. Kempny A, Diller GP, Orwat S, Kaleschke G, Kerckhoff G, Bunck AC et al (2012) Right ventricular-left ventricular interaction in adults with Tetralogy of Fallot: a combined cardiac magnetic resonance and echocardiographic speckle tracking study. Int J Cardiol 154:259–264
22. di Salvo G, Pacileo G, Limongelli G, Verrengia M, Rea A, Santoro G et al (2007) Abnormal regional myocardial deformation properties and increased aortic stiffness in normotensive patients with aortic coarctation despite successful correction: an ABPM, standard echocardiography and strain rate imaging study. Clin Sci (Lond) 113:259–266
23. Young AA, Cowan BR, Occleshaw CJ, Oxenham HC, Gentles TL (2002) Temporal evolution of left ventricular strain late after repair of coarctation of the aorta using 3D MR tissue tagging. J Cardiovasc Magn Reson 4:233–243
24. Laser KT, Haas NA, Jansen N, Schäffler R, Palacios Argueta JR, Zittermann A, Peters B, Körperich H, Kececioglu D (2009) Is torsion a suitable echocardiographic parameter to detect acute changes in left ventricular afterload in children? J Am Soc Echocardiogr 22:1121–1128
25. Dinh W, Nickl W, Smettan J, Kramer F, Krahn T, Scheffold T et al (2010) Reduced global longitudinal strain in association to increased left ventricular mass in patients with aortic valve stenosis and normal ejection fraction: a hybrid study combining echocardiography and magnetic resonance imaging. Cardiovasc Ultrasound 8:29
26. Aurigemma GP, Silver KH, Priest MA, Gaasch WH (1995) Geometric changes allow normal ejection fraction despite depressed myocardial shortening in hypertensive left ventricular hypertrophy. J Am Coll Cardiol 26:195–202
27. Anversa P, Beghi C, Kikkawa Y, Olivetti G (1986) Myocardial infarction in rats. Infarct size, myocyte hypertrophy, and capillary growth. Circ Res 58:26–37
28. Marcus ML, Harrison DG, Chilian WM, Koyanagi S, Inou T, Tomanek RJ, Martins JB, Eastham CL, Hiratzka LF (1987) Alterations in the coronary circulation in hypertrophied ventricles. Circulation 75:I19–I25
29. Karam R, Healy BP, Wicker P (1990) Coronary reserve is depressed in postmyocardial infarction reactive cardiac hypertrophy. Circulation 81:238–246
30. Safar ME, Levy BI, Struijker-Boudier H (2003) Current perspectives on arterial stiffness and pulse pressure in hypertension and cardiovascular diseases. Circulation 107:2864–2869. doi:10.1161/01.cir.0000069826.36125.b4
31. Vitarelli A, Conde Y, Cimino E, D'Orazio S, Stellato S, Battaglia D, Padella V, Caranci F, Continanza G, Dettori O, Capotosto L (2008) Assessment of ascending aorta distensibility after successful coarctation repair by strain Doppler echocardiography. J Am Soc Echocardiogr 21:729–736. doi:10.1016/j.echo.2007.10.007
32. Biederman RW, Doyle M, Yamrozik J, Williams RB, Rathi VK, Vido D et al (2005) Physiologic compensation is supranormal in compensated aortic stenosis: does it return to normal after aortic valve replacement or is it blunted by coexistent coronary artery disease? An intramyocardial magnetic resonance imaging study. Circulation 112:I429–I436